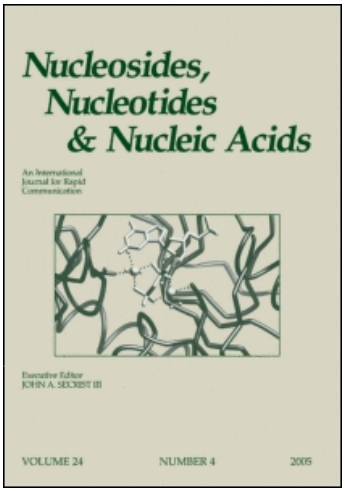

Nucleosides, Nucleotides and Nucleic Acids
Publication details, including instructions for authors and subscription information:
http://www.informaworld.com/smpp/title~content=t713597286

Oxidation Chemistry of Adenosine-3', 5'-Cyclic Monophosphate at Pyrolytic Graphite Eletrode

Rajendra N. Goyal[a]; Anuradha Tyagi[a]
[a] Department of Chemistry, Indian Institute of Technology Roorkee, Roorkee, India

Online publication date: 22 December 2010

To cite this Article Goyal, Rajendra N. and Tyagi, Anuradha(2006) 'Oxidation Chemistry of Adenosine-3', 5'-Cyclic Monophosphate at Pyrolytic Graphite Eletrode', Nucleosides, Nucleotides and Nucleic Acids, 25: 12, 1345 — 1362
To link to this Article: DOI: 10.1080/15257770600918813
URL: http://dx.doi.org/10.1080/15257770600918813

Nucleosides, Nucleotides, and Nucleic Acids, 25:1345–1362, 2006

ISSN: 1525-7770 print / 1532-2335 online
DOI: 10.1080/15257770600918813

Taylor & Francis
Taylor & Francis Group

OXIDATION CHEMISTRY OF ADENOSINE-3′, 5′-CYCLIC MONOPHOSPHATE AT PYROLYTIC GRAPHITE ELETRODE

Rajendra N. Goyal and Anuradha Tyagi □ *Department of Chemistry, Indian Institute of Technology Roorkee, Roorkee, India*

□ *The voltammetric oxidation of adenosine-3′,5′-cyclic monophosphate (3′,5′- CAMP) has been studied in the pH range 2.13–10.07 using pyrolytic graphite electrode (PGE). Voltammetric, coulometric, spectral studies, and product characterization indicate that the oxidation of 3′,5′-CAMP occurs in an EC reaction involving a $6H^+$, 6e process at pH 7.24. Electrooxidized products were seperated by semipreparative high performance liquid chromatography (HPLC) and were characterized by mp, ^{1}HNMR, FTIR, and GC-mass as allantoin cyclic ribose monophosphate and 3 dimers as the major products. A detailed interpretation of the redox mechanism of 3′,5′-CAMP also has been presented to account for the formation of various products.*

Keywords Adenosine-3′,5′-cyclic monophosphate; Adenosine nucleotide; Electrooxidation

INTRODUCTION

Adenosine-3′,5′-cyclic monophosphate (3′,5′- CAMP) is composed of adenine, a nitrogen base in which N_9 position is attached to 3′,5′–cyclic ribose monophosphate group. It is produced in vitro by the glucose metabolism in dental pulp in the presence of various inflammatory chemical mediators like histamine, 5-HT in the medium of prostaglandins (PGE 1 or 2).[1] 3′,5′- CAMP has been reported as the second messenger,[2,3] which can modulate neural excitability.[4] The stimulation of the cyclic adenosine monophosphate second messenger pathway might be a potential strategy for the prevention of vein graft diseases.[5] CAMP plays important roles in cell metabolism, neurotransmission,[6,7] protein formation, cell proliferation,[8] pancreatic secretion,[9] osteoblast regulation,[10] cellular

Received 03 April 2006; accepted 12 June 2006.
One of the authors (A. T.) is thankful to the Council of Scientific and Industrial Research (CSIR) for the award of Research Fellowship. Financial assistance for this work was provided by CSIR, New Delhi, vide grant number F.No. 10-2(5)2003(I)-E.U. II.
Address correspondence to Rajendra N. Goyal, Department of Chemistry, Indian Institute of Technology, Roorkee, Roorkee 247-667, India. E-mail: rngcyfcy@iitr.ernet.in

transformation,[11] and in the development of malignant diseases.[12] It involves in stress-induced metabolic disorders[13] and enhances the synthesis of stress proteins after heat shock,[14] increases the pine pollen tube length during germination.[15] Decreased intracellular CAMP concentration increases the hormonal action of melatonin, acetylcholine, insulin, and prostaglandin.[16] Prostaglandin A1 (PGA 1) increases CAMP concentration in thyroid slices from thyroxine-treated dogs.[17] Cholera toxin (CTx) has been found to elevate the level of CAMP in the differentiated promyelomonocytic cell line U 937.[18]

The electrochemical oxidation of adenosine[19] has been reported from this laboratory, however, the products of electrolysis were characterized only on the basis of GC-MS. The electrooxidation of cyclic derivatives of adenosine nucleotides at solid electrodes has not been studied so far. One of the probable reasons for this is the high oxidation potential of these compounds. Therefore, it is considered desirable to study the oxidation of 3′,5′-CAMP at PGE. It is expected that the results will provide useful information on the primary and secondary electrode reactions involved in its metabolism in the human system.

EXPERIMENTAL

Materials

3′,5′-CAMP was obtained from SRL (Bombay, India), and was used as received. N,O-bis(trimethylsilyl)triflouroacetamide and silylation grade acetonitrile were obtained from Sigma (St. Louis, MO, USA). Linear and cyclic sweep voltammetric studies were performed on a BAS (West Lafayette, IN, USA) CV 50 W voltammetric analyzer. Controlled potential electrolysis was carried out in a three compartment cell using a pyrolytic graphite plate (area 6 × 1 cm^2) as working electrode, a cylindrical platinum gauze (1.5 × 5 cm^2) as the auxiliary electrode and a Ag/AgCl/KCl sat electrode as the reference electrode. The pyrolytic graphite electrode (PGE) (~6 mm^2) was prepared in the laboratory by reported method.[20] The surface of the PGE was renewed after recording each voltammogram, by rubbing it with emery paper (C/P-400), cleaning the surface with water and drying onto the tissue paper. As the electrode surface area was changed each time due to the cleaning process, voltammetric measurements were performed in triplicate and an average value of the current is reported.

Voltammograms were recorded in phosphate buffers[21] of pH range 2.13–10.07. UV-Vis spectral studies and kinetic studies of the decomposition of the UV absorbing intermediate were carried using a Perkin–Elmer Lambda 35 UV/Vis spectrophotometer (Wellesley, MA, USA). Lyophilization of the exhaustively electrolysed solution was carried out using lyophilizer lab model (Harison Scientific Instruments Co., Delhi, India).

Thin layer chromatography was carried out using glass plates coated with silica gel-G using methanol + benzene (20:80) solvent system. The separation of products was achieved by using Agilent 1100 series HPLC equipped with C-18 reversed phase column (7.8 × 300 mm) attached to a precolumn.

FT-IR spectra of the products were recorded on a Perkin Elmer 1600 series FT-IR spectrophotometer using KBr pellets. GC-MS studies were carried out on a Clarus 500 GC-Mass spectrometer (Perkin Elmer). The ^{1}HNMR spectra of the products were recorded in appropriate deuteriated solvent (CD_3OD, D_2O) with TMS as internal standard by using Avance 500 Digital NMR from Brucker.

Procedure

A stock solution of 3′,5′-CAMP (2.0 mM) was prepared using doubly distilled water. Solutions for voltammetric determinations were prepared by mixing 2 mL of the stock solution and 2 mL of the phosphate buffer of desired pH, so that the effective ionic strength of the solution would be 0.5 M. The solutions were deoxygenated by bubbling nitrogen gas for 8–10 minutes before recording the voltammograms.

UV-Vis spectral changes associated with electron transfer of 3′,5′-CAMP were monitored by applying a potential corresponding to oxidation peak I_a. Of the electrolyzed solution, 2–3 mL was withdrawn at different times in a quartz cell from the working compartment of the H-cell and the spectrum was recorded. When absorbance at λ_{max} reduced to about 50%, electrolysis was turned off by open circuit relaxation, and spectral changes were monitored at different time intervals to detect the UV-Vis absorbing intermediate generated. The kinetics of decay of the UV-Vis absorbing intermediate also was monitored when λ_{max} reduced to about 50% by recording change in absorbance with time at selected wavelengths. The values of rate constant k of the decay of intermediates generated were calculated from the linear log ($A\text{-}A_\alpha$) versus time plots.

The products of the electrooxidation of 3′,5′-CAMP were characterized at pH 7.24. For the identification of oxidation products, about 20–25 mg of 3′,5′-CAMP dissolved in 160 mL of phosphate buffer (μ = 0.2 M) of pH 7.24 was exhaustively electrolyzed at a large PGE at peak potential (E_p) of oxidation peak. The progress of electrolysis was monitored by recording spectra at different time intervals. When the absorbance at the maximum in the spectrum completely disappeared, the exhaustively electrolysed solution was removed from the cell and lyophilized. The colourless material obtained after freeze-drying was extracted with methanol (3 × 10 mL) and the methanolic extract was concentrated to get the products. TLC of the freeze-dried material using benzene + methanol (80:20) indicated presence of four products with R_f values ~0.44, 0.48, 0.53, and 0.61, respectively. The lyophilized material was then dissolved in 2 mL

of methanol (HPLC grade), filtered using HPLC grade filter paper (4 μm) and 500 μL solution was injected in HPLC. The mobile phase used for HPLC experiment was composition of methanol (A) and water (B) at a flow rate of 1.2 mL/minute and the absorbance of the eluents were measured at 260 nm. The gradient system of mobile phase used was as follows, 100% B for the time interval 0–4 minutes, 90% B for 5–8 minutes, 80% B for 9–12 minutes, 75% B for 13–16 minutes, 60% B for 17–20 minutes, and 50% B for 21–22 minutes. The column was equilibrated with 100% B for 10 minutes before the next injection was made. The HPLC chromatogram exhibited a small peak at R_t ~8.309 min (Peak A) and 3 major peaks at R_t ~9.195, 9.845, and 11.828 minutes (peaks B, C, and D). The materials eluted under the small peak was never sufficient to permit its characterization. The volumes eluted under peaks B, C, and D were collected separately after making several injections. The volumes were lyophilized and characterized by mp, IR, ^{1}HNMR. The molar masses of the products were determined after converting them to their thermally stable trimethylsilyl derivatives. For carrying out GC-mass studies (EI mode: 70 eV), the product (~50 μg) was treated with BSTFA-acetonitrile (100 μL each) in a sealed 3 mL vial and heated at 110°C for 10–15 minutes in an oil bath. The vial was then cooled to room temperature and 1 μL was then injected in GC-mass spectrometer. To further support the obtained molar mass in the second set of silylation, the temperature was increased to 140°C which caused removal of 3′,5′-cyclic ribose phosphate units in the products.

RESULTS AND DISCUSSION

Voltammetric studies

Linear sweep voltammetric studies of 1.0 mM 3′,5′-CAMP exhibited one well-defined anodic peak I_a in the entire pH range of 2.13–10.07 at a sweep rate of 20 mVs^{-1}. The peak potential of the peak I_a was found to be dependent on pH and shifted to less positive potentials with increasing pH. The values of the peak current corresponding to peak I_a, however, remained practically constant in the entire pH range. The linear dependence of the peak potential (E_p) on pH can be represented by the relation

$$E_p(I_a)[\text{pH}2.13 - 10.07] = [1547.8 - 34.52\,\text{pH}]\text{mV versus Ag/AgCl}$$

having correlation coefficient of 0.961.

In cyclic sweep voltammetry, 3′,5′-CAMP at a sweep rate of 100 mVs^{-1} exhibited a well-defined oxidation peak I_a, when the sweep was initiated in the positive direction. In the reverse sweep, no cathodic peak was obtained. In the second sweep toward positive potential, a new anodic peak II_a appears

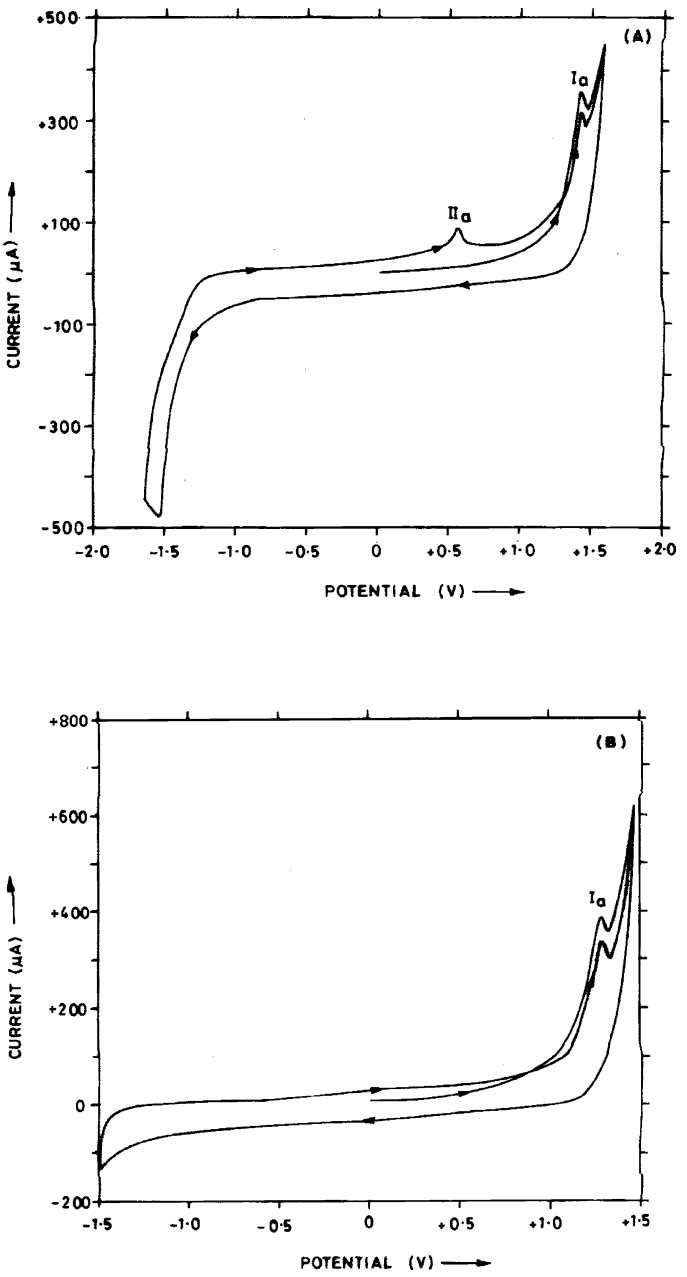

FIGURE 1 Cyclic voltammograms of 1.0 mM 3′,5′-CAMP at a sweep rate of 100 mVs^{-1} at (a) pH = 3.33 (b) pH = 7.24.

in the acidic pH range at less positive potential than E_p of peak I_a and peak Ia still appeared, which shows that electrode did not block after one scan. Peak II_a did not appear at pH 5.10. Typical cyclic voltammograms of 3′,5′-CAMP are presented in Figure 1. The E_p of peak also was dependent

on pH and shifted to less positive potential with increase in pH. The pH dependence of peak potential of peak II_a can be represented as

$$E_p(II_a)[\text{pH } 2.13 - 5.11] = [723.13 - 41.628\,\text{pH}]\,\text{mV versus Ag/AgCl}$$

having correlation coefficient 0.996.

The peak current (i_p) for peak I_a increased linearly with increasing concentration of 3′,5′-CAMP in the range 0.01–0.7 mM at pH 7.24. At concentrations >0.7 mM, the peak current became almost constant. This behavior is supportive of involvement of adsorption complications[22,23] at the PGE electrode surface during reactions involving 3′,5′-CAMP. The adsorption complications were further confirmed by monitoring the change in peak current (i_p) with increase in sweep rate (ν). The i_p of peak I_a was found to be linearly dependent on sweep rate (ν) and can be represented as

$$i_p(\mu A) = [111.91 + 0.9391v(\text{mVs} - 1)]$$

having correlation coefficient 0.987.

The value of E_p also shifted toward more positive potentials with increasing sweep rate. The plot of E_p versus log ν was linear and followed the equation E_p (mV) = 1127.6 + 83.615 log ν, where ν is in mVs^{-1}, with a correlation coefficient of 0.981. This behavior was consistent with the EC nature of the electrode reaction in which the electrode reaction is coupled with with an irreversible follow-up chemical step. [24]

Coulometric studies

As the Ep of the oxidation peak Ia was close to background, the controlled potential electrolysis of 3′,5′-CAMP was carried out at an exact peak potential (E_p) at pH 7.24. The peak currrent (i_p) was found to decrease exponentially with time. The plot of log i_p versus time was straight line for the first 15 minutes of electrolysis after which a large deviation from the straight line was noticed. Such a behavior indicated involvement of competitive chemical reactions.[25] The value of 'n' for the 3′,5′-CAMP was found to be 5.94 ± 0.5 in the entire pH range. Slightly higher deviation in n-values observed is due to large background corrections required.

Spectral studies

The UV spectra of 0.2 mM solution of 3′,5′-CAMP exhibited two well defined λ_{max} at 210 and 260 nm along with a shoulder at 300 nm. Curve 1 in Figure 2 is the initial spectrum of 3′,5′-CAMP just before electrooxidation. Upon application of peak potential 1.39 V, the absorbance systematically decreased in the region 242–280 nm (curves 2–9). However, the absorbance increased systematically in the regions 218–240 and 283–400 nm (curves

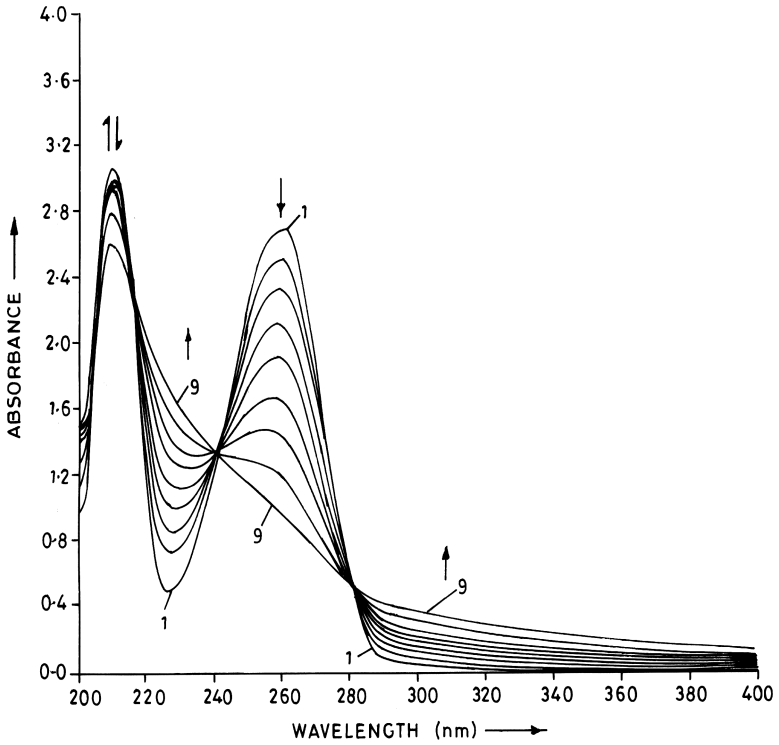

FIGURE 2 Observed spectral changes during the electrochemical oxidation of 0.2 mM 3′,5′-CAMP at pH 7.24 at E_p; spectra recorded at successive intervals of: (a) 0 (b) 5 (c) 10 (d) 10 (e) 15 (f) 15 (g) 30 (h) 30 (i) 60 minutes of electrolysis.

2–9). The absorbance in the region 200–215 nm first increased (curves 1–5) and then decreased (curves 6–9). Three isosbestic points were observed at 218, 240, and 280 nm. The spectral changes observed during electrooxidation of 3′,5′-CAMP at pH 5.11 and 9.23 were essentially similar to that observed at pH 7.24.

In a separate experiment, the applied potential was disconnected by open circuit relaxation when the absorbance λ_{max} reduced to 50% (refer to curve 5 in Figure 5) and the spectral changes at different times were then monitored to detect the wavelength region in which the UV-Vis absorbing intermediate is generated. It was found that the absorbance at the wavelengths 225, 260, and 300 nm decreased on open circuit relaxation. The resulting absorbance versus time plots were found to be exponential in nature (Figure 3). The values of pseudo first order rate constant k were determined at different pH, using log ($A-A_\alpha$) versus time plots (inset in Figure 3). The values of k calculated at different pH and wavelengths are presented in Table 1 and it is noticed that the k values did not show a significant variation with increase in pH. Thus, it is concluded that the same UV-Vis absorbing intermediate is generated in the entire pH range.

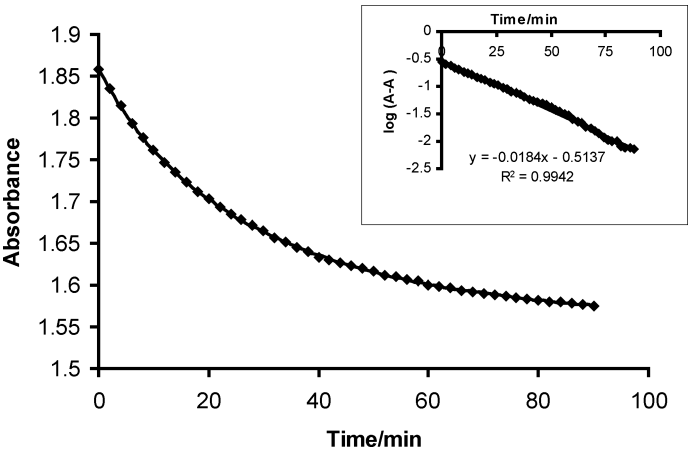

FIGURE 3 Observed plot of absorbance versus time and log (A-A_α) Vs time (inset) for the decay of the UV-absorbing intermediate generated during the electrooxidation of 0.2 mM 3′,5′-CAMP at pH 7.24.

PRODUCT CHARACTERIZATION

The ultimate products of electrooxidation of 3′,5′-CAMP were separated by HPLC and characterized at pH 7.24. The HPLC chromatogram showed 3 major peaks B, C, D at R_t ~9.195, 9.845, 11.828 minutes and a minor peak A at R_t ~ 8.309 minutes respectively, as shown in Figure 4.

(i) Liquid Chromatography Component B

The volume collected under liquid chromatography component **B** (R_t ~9.195 minute) on lyophilization gave white colored powder. The GC-MS studies of this component after silylation at 110°C gave a single peak at R_t ~15.60 minutes, which corresponded to intense molecular ion peak

TABLE 1 Observed pseudo first order rate constants for the decomposition of UV/vis absorbing intermediate during the electrooxidation of 3′,5′-CAMP

pH	λ (nm)	$(k/10^{-3})\ s^{-1}$
5.11	225	0.522
	260	0.606
	300	0.522
7.24	225	0.507
	260	0.640
	300	0.683
9.23	225	0.553
	260	0.513
	300	0.653

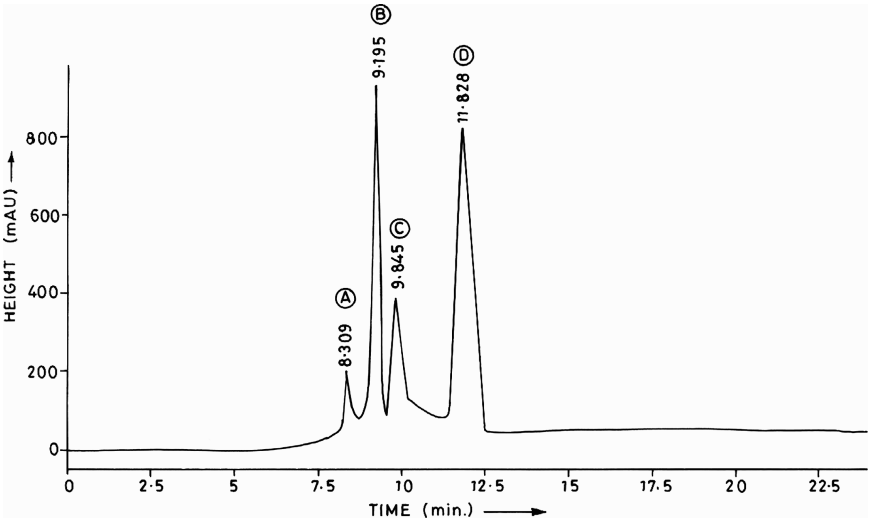

FIGURE 4 HPLC chromatogram of the product mixture obtained following controlled potential electrooxidation of 3′,5′-CAMP at pH 7.24.

at m/z = 784. If silylation is carried out at higher temperature (~140°C) an intense molecular ion peak at m/z = 518 (M^+; 5.12%, peak at R_t ~14.01 minutes) is observed. A loss of m/z 266 by silylation at 140°C indicates that 3′,5′-cyclic ribose monophosphate unit has been detached from the product. The material, thus, is believed to be allantoin and the m/z 784 is due to cyclic 3′,5′-allantoin ribose monophosphate **(11)**. The material had a mp 242°C and ^{1}HNMR spectrum of the material exhibited signals at δ = 5.26 (d, 1 H); 5.6 (s, 2 H); 6.88 (d, 1 H); 8.02 (s, 1 H) and multiplets are obtained in the range of δ = 1.059–2.204 and 3.466–4.724 corresponding to the 8 protons of cyclic ribose monophosphate unit. It, thus, is concluded that the material eluted under chromatographic peak **B** is allantoin containing cyclic ribose monophosphate unit, which has 5 silylable sites. Hence, after silylation it exhibited a molar mass of 784 (M^+).

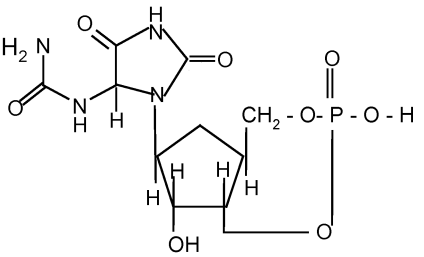

(11)

TABLE 2 Relative abundances and area under peaks observed for various fragments of the peaks in the GC-MS chromatogram of the electrooxidation of 3′,5′-CAMP at pH 7.24

Rt	m/z	Relative abundance of different fragments	Compound identified	Peak area
6.31	877 $(M+H^+)$ (7.17%)	805 (3.67%; $(M+H^+)-(H_2C{=}SiMe_2)$), 777 (2.42%; 805–CO), 788 (2.58%; $(M+H^+)-(O\text{-}SiMe_3)$), 748 (5.33%; 788–$(CN_2)$), 676 (2.21%; 748–$(H_2C{=}SiMe_2)$), 604 (4.56%; 676–$(H_2C{=}SiMe_2)$)	**(15)**	1587029
9.56	733 $(M+H^+)$ (5.10%)	661 (1.70%; $(M+H^+)-(H_2C{=}SiMe_2)$ 589 (6.00%; 661–$(H_2C{=}SiMe_2)$) 376 (3.54%; 589–$(C_2N_3H(SiMe_3)_2)$, 367 (6.65%; $(M+H^+)-(C_5N_5OH(SiMe_3)_3)$, 223 (3.34%; 367–2$(H_2C{=}SiMe_2)$)	**(22)**	1120382
15.60	784 (M^+) (8.67%)	756 (3.12%; M^+–CO), 684 (6.94%; 756–$(H_2C\text{-}SiMe_2)$), 611 (3.73%; 684–$SiMe_3$), 444 (3.13%; $M^+-(SiMe_3\text{-}OH)-(C_5O_5PH_6SiMe_3)$, 416 (4.49%; 444–CO)	**(11)**	5489209
15.74	700 (M^+) (9.90%)	628 (9.50%; $M^+-(H_2C{=}SiMe_2)$), 415 (2.54%; 628–$(C_2N_3H(SiMe_3)_2)$), 350 (5.46%; 415–(C_3N_2H)), 627 (6.50%; M^+–$SiMe_3$), 455 (8.00%; 627–$(N(SiMe_3)_2)C$), 242 (4.95%; 455–$(C_2N_3H(SiMe_3)_2)$)	**(18)**	1188666

(ii) Liquid Chromatography Component C

The component **C** eluted in HPLC at R_t ~9.845 minutes was white colored powder and had a mp of 292°C. The GC-MS of this component after silylation with silylating reagent BSTFA/acetonitrile exhibited a single peak in GC-MS chromatogram (R_t ~15.74 minutes), which corresponded to intense molecular ion (M^+) peak at m/z = 700 (9.90%). The high molar mass indicated the possibility of formation of dimer of adenosine. This dimer appears to be formed by the dimerization of C-8 radical **(13)** to give C-C linked dimer **(18)**. It has 6 silylable sites, which can undergo silylation and the replacable hydrogens on silylation in this molecule will lead to a molar mass of m/z = 700 (M^+) as observed. The high mass peaks observed in the fragmentation pattern are presented in Table 2 and can be explained as shown in Scheme 3. The IR spectrum of this material gave important bands at 3710 (N-H); 1462 (C-H); 1252 (C-C); 1022 (C=N) and 820 (C-N) cm^{-1}. The ^{1}HNMR spectrum of this material exhibited signals at δ = 8.036 (s, 2H, 2 × NH_2), 7.042 (s, 1H, 2 × N_9H), and 5.878 (s, 1H, 2 × C_2H) and, thus, confirmed the product as C-C linked dimer.

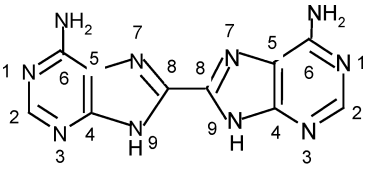

(18)

(iii) Liquid Chromatography Component D

The volume collected under liquid chromatography component **D** (Figure 4) on lyophilization gave a white powder which had a mp of 286°C. The GC-MS of this component after silylation with silylating reagent gave a single peak (R_t ~6.31 minutes), which corresponded to intense peak m/z = 877 ($M+H^+$; 7.17%). The molar mass of 876 suggests the formation of a C_8-$C_{8'}$ linked dimer **(15)** of 2-hydroxy derivative of adenosine. This dimer **(15)** has 8 silylable sites, which can undergo silylation with BSTFA/acetonitrile. The replacable hydrogens on silylation in this molecule will lead to a molar mass of m/z = 877 as observed for this material. The IR spectrum of this material showed important bands at 3708 (N-H); 3400 (O-H); 1250 (C-C); 1016 (C=N) and 809 (C-N) cm^{-1}. The ^{1}HNMR spectrum of this material exhibited signals at $\delta = 8.069$ (s, 2 H, 2 × NH_2), 7.794 (s, 1 H, 2 × OH) and 7.212 (s, 1 H, 2 × N_9H) and thus, confirmed the product **15**.

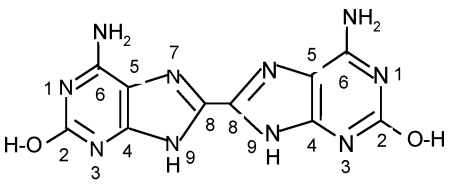

(15)

(iv) Liquid Chromatography Component A

The HPLC peak was relatively small and the material collected under this peak was never enough to permit its complete characterization. The GC-MS studies of this component after silylation gave a single peak in chromatogram at R_t ~9.56 minutes, having m/z 733 ($M+H^+$; 5.10%) and indicated the formation of -O··O- linked dimer **(22)**. The presence of peroxide group in the dimer also was confirmed by the test suggested in the literature [26,27] in which 1.0 mL of 10% acidified potassium iodide solution was added to a small amount of the product. A few drops of starch solution were then added and a blue black color was observed in ~1 minute. This dimer is likely to be formed by the dimerization of C-8 oxygen free radical **(20)**. The dimer (**22**) has 6 silylable sites, which can undergo silylation with

silylating agents. The silylation of replacable hydrogens of **(22)** give a molar mass of 732.

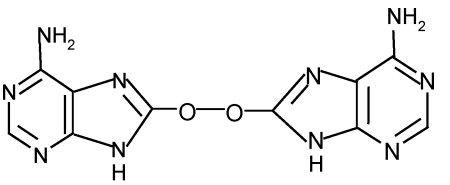

(22)

The peak area observed for different molar mass peaks in GC-MS chromatogram (Table 2) also indicated that the major product of the electrode reaction is allantoin having cyclic ribose monophosphate unit attached to it.

REDOX MECHANISM

The characterization of the observed products formed by the oxidation of 3′,5′-CAMP clearly suggests that the electrooxidation of CAMP is complex and does not follow a simple path. Scheme 1 suggests the major pathway in which breakdown of pyrimidine ring occurs leading to the formation of allantoin 3′,5′-cyclic ribose monophosphate. However, the oxidation also occurs in side reactions involving the free radical formation. The combination of free radicals generated leads to the formation of several dimers.

The initial step in Scheme 1 appears to involve the oxidative hydrolysis of 3′,5′-CAMP **(1)** to produce 2-hydroxy derivative **(2)**. Formation of 2-hydroxy adenine has been well documented during the electrooxidation of adenine and hydroxyadenine.[28] Thus, it seems reasonable to conclude that initial oxidation would occur at position-2 to give 2-hydroxy derivative **(2)**. Further $2H^+$, 2e oxidation of 2-hydroxyadenine derivative **(2)** will give 2,8-dihydroxy derivative **(3)**. The oxidation of 2,8-dihydroxy derivative is expected to be easier due to presence of 2 hydroxyl groups. Thus, further $2H^+$, 2e oxidation of **(3)** then gives a diimine species **(4)**. One would expect that $2H^+$, 2e oxidation peak of 2,8-dihydroxy derivative also should be observed in cyclic voltammograms. However, no peak for this oxidation step was noticed. The probable reason for this behavior could be easier oxidation of 2,8-dihydroxy derivative, which is likely as it immediately oxidizes as soon as it is formed. The formation of diimine species is common and has been reported during oxidation of various purines.[29] The increase in absorbance in the region 283–400 nm during spectral studies appears to be due to the formation of diimine **(4)**. It already has been reported in the literature that diimine generated during oxidation of purines had a

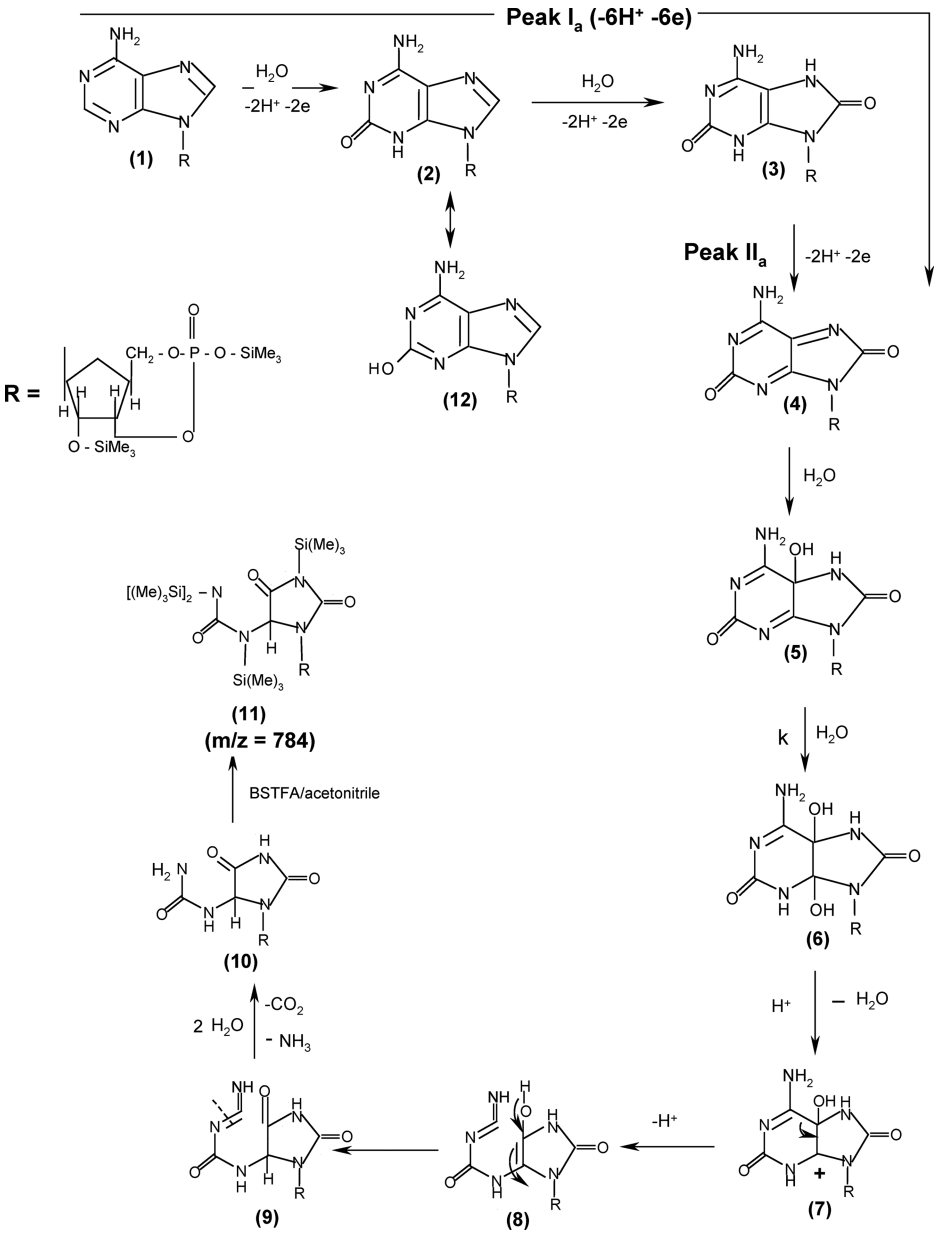

SCHEME 1

short half life (~40 ms) at different electrods,[30,31] Hence, due to unstable nature it readily get attacked by water molecules to give 4,5-diol species (**6**). The attack of first water molecule on the diimine[28] would occur almost instantly because of the unstable nature of diimine to give imine alcohol (**5**). However, the attack of second water molecule would be slow and the decay

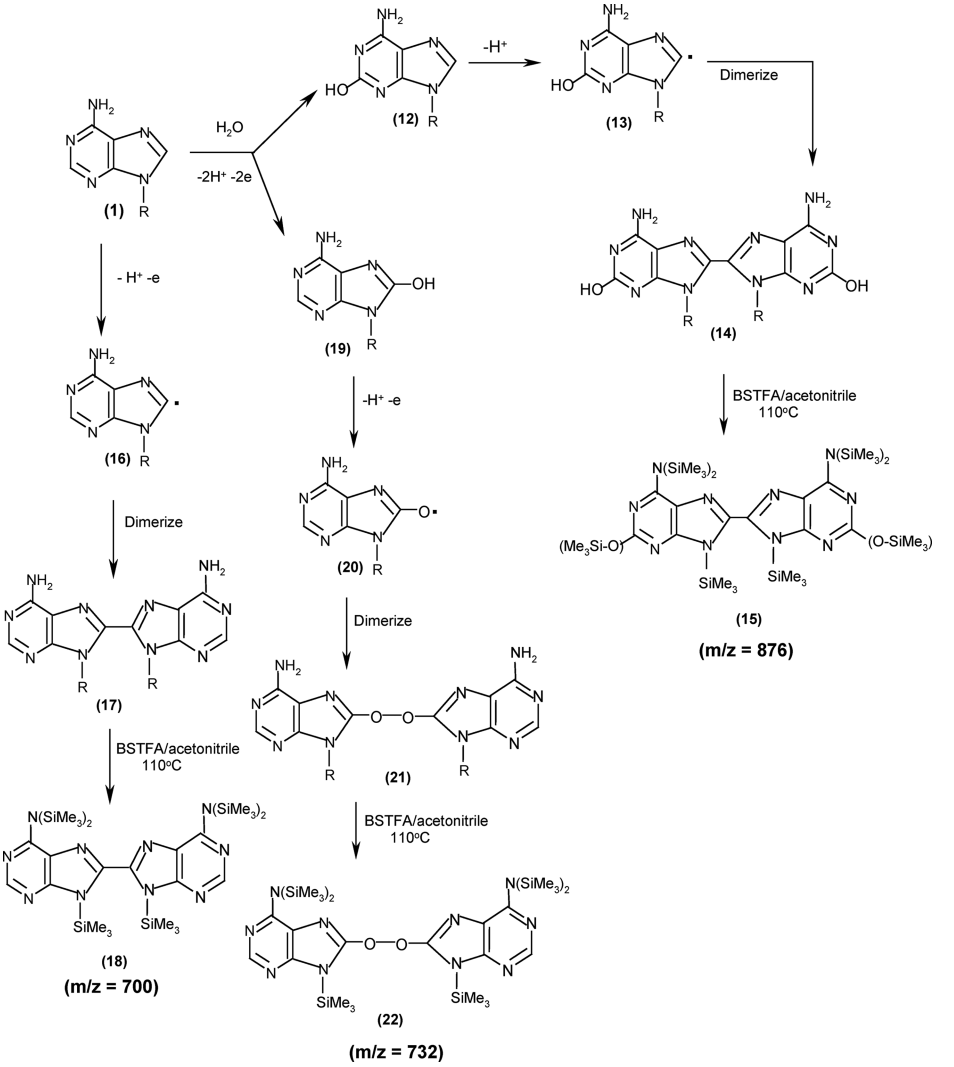

SCHEME 2

of imine alcohol[32] to give 4,5-diol has been monitored spectrophotometrically, and this step represents the value of k determined experimentally from log (A-A_α) versus time plots. Attack of H^+ and simultaneous loss of H_2O molecule from **(6)** leads to the formation of carbocation **(7)**. Removal of H^+ from NH_2 will then generate specie **(9)**. Further attack of water will lead to the generation of the ultimate product allantoin 3′,5′-cyclic ribose monophosphate **(11)** along with CO_2 and NH_3. The formation of allantoin has been confirmed by ^{1}HNMR, IR, and GC-MS studies.

The oxidation of 2-hydroxy 3′,5′-CAMP **(12)** also proceeds through a side reaction in which 1 H^+, 1e oxidation generates C-8 radical specie **(13)**, which

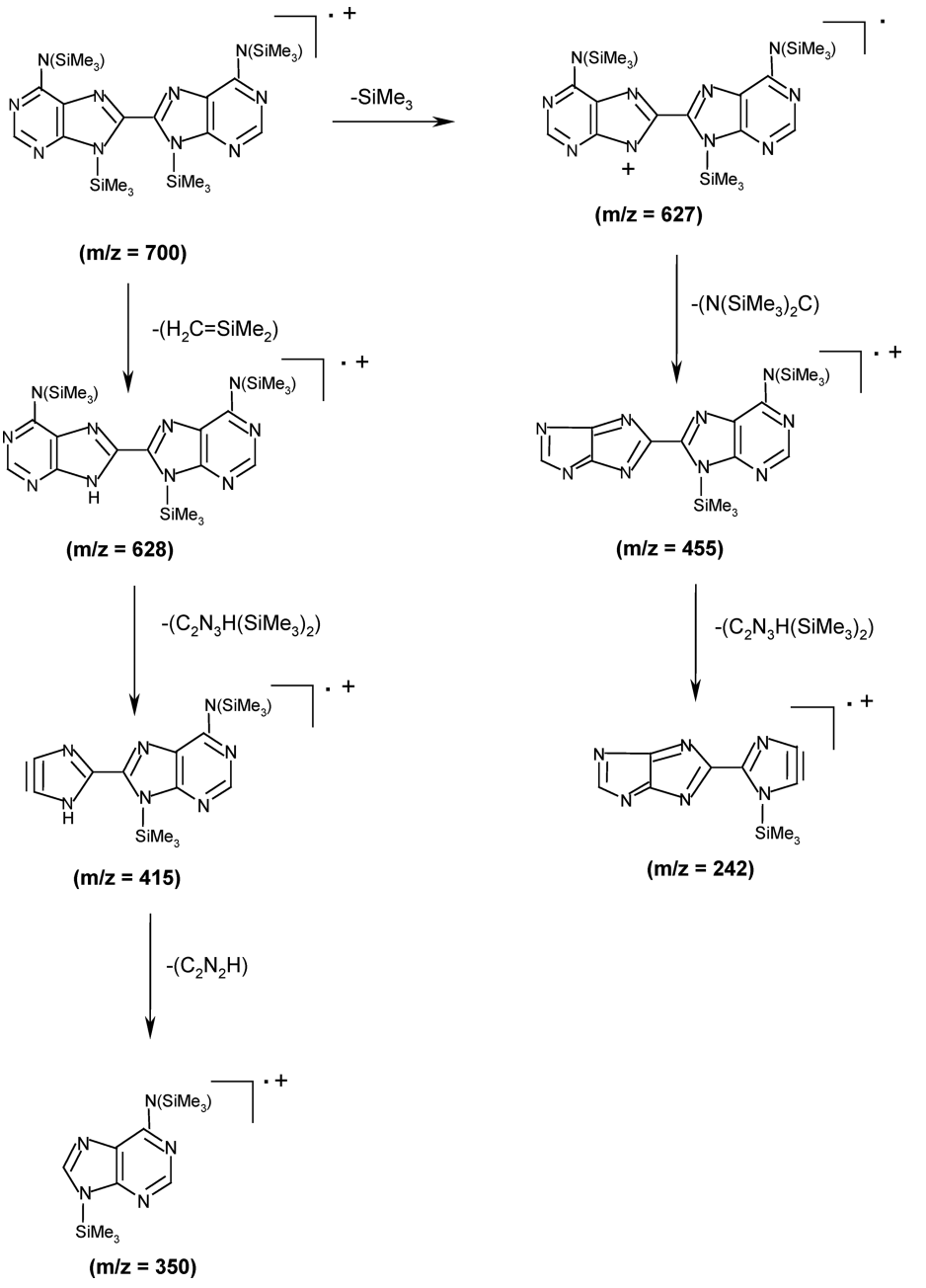

SCHEME 3

rapidly undergoes dimerization and leads to the formation of C-C linked dimer **(14)**. The dimer **(14)** on silylation exhibited a molar mass peak at m/z = 876 (R_t ~6.31 minutes) corresponding to 8 position silylated of **(14)**. Our results also indicate that the initial 2 H^+, 2e oxidation of compound

TABLE 3 Peak potential (E_p) of oxidation peak I_a of various adenine compounds at pH 7.2

Compound	E_p (mV)
Adenine	950
Adenosine	1150
Adenosine monophosphate (AMP)	1200
3′,5′-Cyclic adenosine monophosphate (3′,5′-CAMP)	1298

1 leads to the formation of 2-hydroxy as well as 8-hydroxy derivative. The formation of such derivatives during electrochemical as well as enzymic oxidation of purines have already been reported in the literature.[28,33,34] Thus, simultaneous formation of both 2-hydroxy and 8-hydroxy derivatives takes place during the electrooxidation of 3′,5′-CAMP. 1 H^+, 1e oxidation of **(19)** produces an oxygen free radical **(20)**, which undergoes dimerization and resulted in the formation of peroxide linked dimer **(21)**. The peroxide linked dimer **(21)** on silylation exhibited a molar mass peak at $m/z = 732$ (R_t ~9.56 minutes). The formation of C_8-$C_{8'}$ linked dimer **(17)** can be explained by 1 H^+, 1e oxidation of 3′,5′-CAMP **(1)** to give C-8 radical **(16)**. Such a removal of an electron from position −8 is well documented during oxidation of purine nucleoside.[35] The free radical **(16)** dimerizes rapidly to give C-C linked dimer **(17)**. The formation of dimer **(17)** was confirmed by ^{1}HNMR, IR and GC-MS studies.

3′,5′-CAMP appears to follow a complex electrooxidative mechanism in comparison to its base adenine and nucleoside and nucleotide, that is, adenosine and adenosine monophosphate, which is probably due to very high positive potential of its oxidation as shown in Table 3. A comparison of electrooxidation behavior of adenosine monophosphate (AMP) and 3′,5′-CAMP also has been made to evaluate the effect of cyclic ribose phosphate moiety on ease of oxidation. As the peak potential of AMP is lesser than 3′,5′-CAMP, the applied potential during the controlled potential electrolysis (CPE) of AMP is ~100 mV less than 3′,5′-CAMP (Table 3). In both the cases, the applied potential in CPE is close to background and it is likely that water oxidation reactions might have favored free radical pathways in both the cases leading to the formation of dimeric products. The nature and number of dimers formed depend on the stability of free radicals generated. In the case of 3′,5′-CAMP the peak potential is very high and the course of oxidation proceeds in 2 parallel pathways leading to the formation of 3 dimers and allantoin-3′,5′-cyclic ribose mono phosphate, which have been characterized by FT-IR, ^{1}HNMR, and GC-MS studies. Whereas, in the case of AMP only 5 dimeric compounds are observed[36] that have been characterized using only GC/MS. The dimer **(15)** is the only common product formed in both the cases whereas other products are different in the mode of combination of radicals during dimer formation. One of

the probable reasons for this difference is the presence of bulky cyclic ribose monophosphate unit, which does not permit dimer formation due to steric hindrance particularly through C_8-C_8 position. One would expect that the cyclic ribose monophosphate unit should hydrolyze during oxidation, however, these studies clearly show that this ring is sufficiently stable and remain attached with allantoin ring.

CONCLUSIONS

These studies clearly reveal that the electrooxidation of 3′,5′-CAMP proceeds via 2 parallel pathways leading to the formation of three dimers and the major product as an allantoin cyclic ribose monophosphate. More than one pathway are always possible for such reactions. The formation of purine dimers and oligomers in the human system due to abnormal oxidation of parent compounds already has been reported.[37,38] Such compounds have been claimed responsible for various diseases. Therefore, it is expected that these electrochemical studies will throw light on the possible role of 3′,5′- CAMP in human system.

REFERENCES

1. Kiyohara, H. Studies on the relation between glucose metabolism and c- AMP formation in dental pulps in the presence of inflammatory chemical mediators in vitro. *J. Meikai Univ. School of Dentistry* **1989**, 18, 171–186.
2. Coutifaris, C.; Omigbodun, A.; Coukos, G. The fibronectin receptor a5 integrin subunit is up-regulated by cell-cell adhesion via a cyclic AMP dependent mechanism: Implications for human trophoblast migration. *American J. Obst. Gyn.* **2005**, 192, 1240–1253.
3. Gellersen, B.; Brosens, J. Cyclic AMP and progesterone receptor cross-talk in human endometrium: a decidualizing affair. *J. Endocrinol.* **2003**, 178, 357–372.
4. Shaikh, A.G.; Finlayson, P.G. Excitability of auditory brainstem neurons, in vivo, is increased by cyclic–AMP. *Hearing Research* **2005**, 201, 70–80.
5. Sakaguchi, T.; Asai, T.; Belov, D.; Okada, M.; Pinsky, D.J.; Schmidt, A.M.; Naka, Y. Influence of ischemic injury on vein graft remodeling: role of cyclic adenosine monophosphate second messenger pathway in enhanced vein graft preservation. *J. Thor. Cardiovasc. Surg.* **2005**, 129, 129–137.
6. Rall, T.W. On the importance of cyclic AMP in neurobiology: an essay. *Metab. Clin. Exp.* **1975**, 24, 241–247.
7. Wissler, J.H.; Stecher, V.J.; Sorkin, E. Cyclic AMP and chemotaxis of leukocytes. *Cyclic AMP, Cell Growth, Immune Response, Proc. Symp.* **1974**, 270–283.
8. Carenzi, A. The role of cyclic nucleotides. *Rivista di Farmacologia e Terapia* **1976**, 7, 511–520.
9. Francavilla, A.; Pansini, F.; Centonze, V.; Dicillo, M.; Albano, O.; Fasano, V. Importance of cyclic AMP on the regulation of pancreatic secretions in man. *Atti e Relazioni—Accademia Pugliese delle Scienze Part 2* **1973**, 31, 276–275.
10. Yamamoto, T.; Gay, C.V. Ultrastructural localization of adenylate cyclase in chicken bone cells. *J. Histochem. Cytochem.* **1989**, 37, 1705–1709.
11. Johnson, G.S. The importance of cyclic AMP in cellular transformation. *Cyclic Nucleotide Dis. Proc. Symp.* **1975**, 35–44.
12. Williams, A.C. The importance of cyclic nucleotides (cyclic GMP and cyclic AMP) in the development of malignant disease. *Diss. Abstr. Int. B* **1988**, 49, 1100.
13. Stremmel, W. Importance of cyclic AMP in stress-induced metabolic disorders. *Fed. Rep. Ger. Infusionstherapie* **1973**, 1, 36–40.

14. Pizurki, L.; Polla, B.S. cAMP modulates stress protein synthesis in human monocytes macrophages. *J. Cell. Physiol.* **1994**, 161, 169–177.
15. Dhawan, A.K.; Malik, C.P. Cyclic AMP control of some oxido-reductases during pine pollen germination and tube growth. *Phytochemistry* **1979**, 18, 2015–2017.
16. Schultz, G. Importance of cyclic AMP with hormonal effect. *Internist* **1972**, 13, 159–166.
17. Dekker, A.; Field, J.B. Correlation of effects of thyrotropin, prostaglandins, and ions on glucose oxidation, cyclic AMP, and colloid droplet formation in dog thyroid slices. *Metab. Clin. Exp.* **1970**, 19, 453–464.
18. Fischer, T.; Zumbihl, R.; Armand, J.; Casellas, P.; Rouot, B. Prolonged elevation of intracellular cyclic AMP levels in U937 cells increases the number of receptors for and the responses to formylmethionyl-leucyl-phenylalanine, independently of the differentiation process. *Fr. Biochem. J.* **1993**, 311, 995–1000.
19. Goyal, R.N.; Sangal, A. Electrochemical investigations of adenosine at solid electrodes. *J. Electroanal. Chem.* **2002**, 521, 72–80.
20. Miller, F.J.; Zittel, H.E. Fabrication and use of pyrolytic graphite electrode for voltammetry in aqueous solutions. *Anal. Chem.* **1963**, 35, 1866–1869.
21. Christian, G.D.; Purdy, W.C. The residual current in orthophosphate medium. *J. Electroanal. Chem.* **1962**, 3, 363–367.
22. Nicholson, R.S.; Shain, I. Theory of stationary electrode polarography. single scan and cyclic methods applied to reversible, irreversible, and kinetic systems. *Anal. Chem.* **1964**, 36, 706–723.
23. Brown, E.C.; Large, R.F. Cyclic volammetry AC polarography and related techniques. In *Physical Methods of Chemistry*, eds. A. Weissberger B. W. Rossiter (Wiley: New York), **1974**, 423–530.
24. Goyal, R.N.; Rastogi, A.; Sangal, A. Electro-oxidation of 6-mercaptopurine riboside with special emphasis on the stability of the dimer in aqueous solutions. *New J. Chem.* **2001**, 25, 545–550.
25. Cauquis, G.; Parker, V.D. Methods for the elucidation of organic electro chemical reactions. In *Organic Electrochemistry*, ed. M.M. Baizer (Marcel Dekker: New York), 1973, 93–154.
26. Furniss, B.R.; Hannaford, A.J.; Smith, P.W.G.; Tatchall, A.R. *Vogel's Textbook of Practical Organic Chemistry* (Longman, Singapore: Singapore), 1994.
27. Swern, D. *Organic Peroxides.* (Wiley Interscience: New York), 1971.
28. Goyal, R.N.; Kumar, A.; Mittal, A. Oxidation chemistry of adenine and hydroxyadenines at pyrolytic graphite electrode. *J. Chem. Soc. Perkin Trans 2* **1991**, 1369–1375.
29. Toth, A.B.; Goyal, R.N.; Wrona, M.Z.; Lacava, T.; Nguyen, N.T.; Dryhurst, G. Electrochemical and enzymic oxidation of biological purines. *Bioelectrochem. Bioenerg* **1981**, 8, 413–435.
30. Goyal, R.N.; Toth, A.B.; Dryhurst, G. Electrochemical and peroxidase-catalyzed redox chemistry of 9-Methyl uric acid. *J. Electroanal. Chem.* **1982**, 133, 287–297.
31. Teresa, E.; Peterson, A.; Toth, A.B. Electrochemical and photochemical oxidation of the deazapurine nucleotide drug tubercidin-5′-monophosphate. *J. Electroanal. Chem.* **1988**, 239, 161–173.
32. Roth, J.S.; Ford, J.J.; Tanaka, M.; Mitsuya, H.; Kelley, J.A. Determination of 2′-β-fluoro-2′,3′-dideoxyadenosine, an experimental anti-AIDS drug, in human plasma by high-performance liquid chromatography. *J. Chromatogr. B; Biomed. Appl.* **1988**, 712, 199–210.
33. Conway, A.C.; Goyal, R.N.; Dryhurst, G. Electrochemical oxidation of hypoxanthine. *J. Electroanal. Chem.* **1981**, 123, 243–264.
34. Brett, C.M.A.; Oliveira Brett, A.M.; Serrano, S.H.P. On the adsorption and electrochemical oxidation of DNA at glassy carbon electrodes. *J. Electroanal. Chem.* **1994**, 366, 225–231.
35. Tyagi, S.K.; Dryhurst, G. Electrochemical oxidation of xanthosine. *J. Electroanal. Chem.* **1987**, 216, 137–156.
36. Goyal, R.N.; Sangal, A. Electrochemical oxidation of adenosine monophosphate at a pyrolytic graphite electrode. *J. Electroanal. Chem.* **2003**, 557, 147–155.
37. Borges, G.; Mendonca, P.; Joaquim, N.; Coucelo, J.; Aureliano, M. Acute effects of vanadate oligomers on heart, kidney, and liver histology in the lusitanian toadfish (Halobatrachus didactylus). *Archives of Environmental Contamination and Toxicology* **2003**, 45 (3), 415–422.
38. Duker, N.J.; Sperling, J.; Soprano, K.J.; Druin, D.P.; Davis, A.; Ashworth, R. β-amyloid protein induces the formation of purine dimers in cellular DNA. *J. Cell. Biochem.* **2001**, 81, 393–400.